

Miscibility of Poly(arylene phosphine oxide) Systems and Bisphenol A Poly(hydroxy ether)

Sheng Wang,[†] Hong Zhuang, H. K. Shobha, T. E. Glass, M. Sankarapandian, Qing Ji, A. R. Shultz, and J. E. McGrath*

Department of Chemistry and Materials Research Institute, Virginia Polytechnic Institute and State University, Blacksburg, Virginia 24061-0344

Received October 23, 2000; Revised Manuscript Received August 29, 2001

ABSTRACT: A number of new aryl phosphorus-containing polymers were found to be miscible with the commercially significant bisphenol A-based poly(hydroxy ether)s (PHE) over the entire composition range by differential scanning calorimetry (DSC) and dynamic mechanical analysis (DMA) measurements of the blends. Both the FTIR and CP-MAS ³¹P NMR results suggested extensive hydrogen-bonding interactions between hydroxyl groups and the phosphonyl groups. Specifically, the poly(arylene thioether diphenylphenylphosphine oxide) and phosphorus-containing polyimides were also miscible with PHE, again emphasizing the importance of phosphonyl groups for generating miscible polymer blends. In contrast, a structurally similar commercial polyimide, Ultem, was not miscible with PHE. These results suggested that the miscibility was induced mainly by hydrogen bonding between phosphonyl and hydroxyl groups, rather than other sites such as carbonyl or ether oxygen atoms and the hydroxyl groups. Furthermore, the measurements of proton spin–lattice relaxation times in the rotating frame (*T*_{1ρ}) showed that the phosphorus-containing polyimide/PHE blends were homogeneous even at about a 4 nm scale.

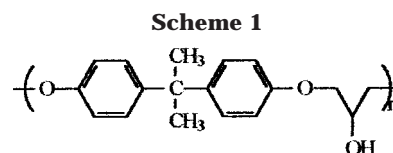
Introduction

Polymer blends have found many industrial applications, since this strategy can often generate relatively inexpensive materials with improved properties. However, most polymer blends are heterogeneous (immiscible). From a thermodynamic point of view, it is well-known that the entropy of mixing increase is very small in polymer blends. But miscibility can often be achieved by a favorable (negative) mixing enthalpy. Further understanding of miscibility and the stability of homogeneous polymer blends is of great interest from both academic and industrial points of view. It has been crucial for the development of new materials, since only the miscible polymer blends are thermodynamically stable.^{1–4} Hydrogen bonding is the most important specific interaction for promoting polymer miscibility.

The literature illustrates that bisphenol A poly(hydroxy ether) (PHE) is miscible with many polymers, because its pendant hydroxyl groups can act as both proton donors and acceptors. The structure of PHE is shown in Scheme 1.

For example, it is miscible with poly(ε-caprolactone),⁵ poly(butylene terephthalate),⁶ a cyclohexane-dimethanol-based polyester,⁷ a polyester-based polyurethane,⁸ poly(ethylene adipate),⁹ poly(butylene adipate), poly(ethylene oxide),¹⁰ poly(vinyl ethyl ether),^{10a} poly(methyl methacrylate),¹¹ poly(vinylpyrrolidone) (PVP),¹² phenolphthalein poly(ether ether ketone),¹³ poly(*N*-methyl-*N*-vinylacetamide) (PMVAc),¹⁴ poly(*N,N*-dimethylacrylamide) (PDMAc),¹⁴ poly(ethyloxazoline) (PEOx),^{14,15} poly(ether sulfone),¹⁶ poly(arylene ether phenylphosphine oxide),^{17,18} and various epoxy resins.¹⁹ All of the polymer blend systems were reported to be miscible over the entire composition region.

In recent years, the discovery of the extensive hydrogen bonding between phosphonyl and hydroxyl groups has sparked new interest in preparing some new



Bisphenol A Poly(hydroxy ether)s “Phenoxy Resin” (PHE)

phosphorus-containing polymers, since the hydrogen-bonding interaction between hydroxyl group and phosphonyl group promotes polymer–polymer miscibility and improves the selected properties.^{17,18,20–22} It also has potential to stabilize nanosilica particle/polymer composites.^{24d}

Introducing interphase or sizing materials has been demonstrated to improve the mechanical properties of composites.²³ In the past decade, many new phosphorus-containing high-performance polymers including poly(arylene ether)s,²⁴ poly(arylene thioether)s,²⁵ polyimides,²⁶ and cyanate resins²⁷ have been synthesized in our laboratory and elsewhere. These polymers exhibit good mechanical properties, thermal stability, and fire and atomic oxygen resistance. Introduction of the phosphonyl group also increases the polarity of the polymers, which allows them to serve as excellent proton acceptors. Incorporating phosphonyl groups may also improve the surface adhesion between these polymers and other materials, organic or inorganic, which have hydroxyl groups. This capability has promoted our interest in the possibility of phosphorus-containing high-performance polymers as interphase materials for composites which have either epoxy resins or bisphenol A dimethacrylate matrices. The major advantages of those high-performance polymers include high *T*_g and good mechanical properties such as toughness. Another objective of our research was to develop some new polymer blends with improved mechanical and thermal properties. Recent research showed that bisphenol A- or hydroquinone-based poly(arylene ether phosphine oxide)s formed miscible blends with bisphenol A-based poly(hydroxy ether) (phenoxy resin) (PHE).^{17,18} Further

[†] Present address: Dow Corning Corporation, Semiconductor Fab Materials, Midland, MI 48686.

* Corresponding author. E-mail jmcgrath@vt.edu.

Table 1. GPC and Intrinsic Viscosity Characterization of Bisphenol A Poly(hydroxy ether)s, Bisphenol A Polysulfone, Poly(ether sulfone), Various Phosphorus-Containing Poly(arylene ether)s, Polyimides, and Ultem

sample	GPC			$[\eta]$ (dL/g) CHCl ₃ , 25 °C
	$M_n \times 10^{-3}$	$M_w \times 10^{-3}$	M_w/M_n	
BPA-PEPO-100	39	74	1.9	0.42
BPA-PEPO-50	70	159	2.3	0.73
HFBPA-PEPO	58	128	2.2	0.67
BP-PEPO	140	281	2.0	2.0 ^a
SS-PTPO	42	92	2.2	0.48
BPADA-DAMPO	20	33	1.8	0.28 ^a
BPADA-DAPPO	19	38	2.0	0.28 ^a
BPADA- <i>m</i> -PDA	20	33	1.7	0.40
Udel	26	48	1.9	0.39
Victrex	21	34	1.6	0.34 ^b
PHE	20	46	2.3	0.28

^a In NMP at 30 °C. ^b In NMP at 25 °C.

work demonstrated that bisphenol A poly(arylene ether phenyl phosphine oxide) is miscible with both oligomeric uncured and cured commercial bisphenol A dimethacrylate networks (vinyl ester resin with styrene as the diluent).²² The hydrogen-bonding interaction between the hydroxyl group and the phosphonyl group was shown to be the driving force for the miscibility. However, miscibility depends on both the favorable specific interaction with the phosphonyl group and the less favorable, or unfavorable, interaction with other groups in the chain. Therefore, miscibility is a compromise of the favorable specific interaction with the phosphonyl groups and unfavorable interactions with other groups in the copolymer chains. Extension of our investigations to some other systems was important to further define the universality of compatibility by phosphonyl/hydroxyl hydrogen bonding. The present research was designed to systematically investigate the miscibility of PHE with phosphorus-containing poly(arylene ether)s, such as 4,4'-(hexafluoroisopropylidene)-diphenol (HFBPA)- or biphenol (BP)-based poly(arylene ether phenylphosphine oxide) (abbreviated as HFBPA-PEPO and BP-PEPO, respectively), with poly(arylene thioether phenylphosphine oxide) (abbreviated as SS-PTPO), and with polyimides (polymers prepared from 2,2'-bis[4-(3,4-dicarboxyphenoxy)phenyl]propane dianhydride (BPADA) and bis(*m*-aminophenyl)methylphosphine oxide (DAMPO) (abbreviated as BPADA-DAMPO) or bis(*m*-aminophenyl)phenylphosphine oxide (DAPPO) (abbreviated as BPADA-DAPPO). The structures of the above polymers and the related systems are shown in Schemes 2 and 3.

Experimental Section

Materials. Bisphenol A poly(hydroxy ether) (PHE) (M_n = 20K) was supplied by Phenoxy Associates, Inc. (Rock Hill, SC). A commercial polyimide, Ultem resin (BPADA-*m*-PDA), was supplied by the General Electric Company. A commercial cycloaliphatic epoxy resin, ERL-4221 (3,4-epoxycyclohexylmethyl-3,4-epoxycyclohexyl carboxylate) (ECHMECHC), was obtained from the Union Carbide Chemicals. Polymers BPA-PEPO, HFBPA-PEPO, and BP-PEPO were prepared in our laboratory.^{18,24} SS-PTPO and BPADA-DAMPO and BPADA-DAPPO polyimides were synthesized in our laboratory.^{25,26} The molecular weights and intrinsic viscosities of these polymers are tabulated in Table 1.

Preparation of Polymer Blends. The BPA-PEPO, HFBPA-PEPO, SS-PTPO, BPADA-DAMPO, and BPADA-DAPPO were separately dissolved in chloroform as 7.5 wt % solutions and

then mixed with portions of a 7.5 wt % PHE chloroform solution to achieve the desired blend compositions. The polymer mixtures were isolated by precipitation in methanol and then dried in a vacuum oven for 24 h at 150 °C. Films for FTIR measurements were prepared by casting blend solutions onto glass slides or salt plates and drying in a vacuum oven in a similar manner. The films used for dynamic mechanical analysis (DMA) measurements were obtained by compression molding between metal plates for about 3 min at temperatures ranging from 160 °C for the PHE to 280 °C for the phosphorus-containing homopolymers. The melt-pressed samples were allowed to cool to ambient temperature between the metal plates.

The polymer blends BPADA-*m*-PDA/PHE and BP-PEPO/PHE were prepared in dimethylacetamide (DMAc) solutions instead of chloroform, but the other procedures were similar. Thermogravimetric analysis (TGA) and nuclear magnetic resonance spectroscopy (NMR) were used to determine that all the solvent was completely removed from the specimen.

Characterization. Intrinsic viscosities were measured in chloroform or *N*-methylpyrrolidone (NMP) at 25 °C. GPC measurements were performed at 60 °C using a Waters 150C instrument to characterize the molecular weights and molecular weight distributions. NMP containing 0.02 M phosphorus pentoxide was the solvent. A differential refractive index detector and a Viscotek differential viscometer connected in parallel permitted calculation of absolute molecular weights and molecular weight distributions by applying the universal calibration principle.²⁸

FTIR measurements were performed with a Nicolet impact mode 400 FTIR spectrometer. Each spectrum was based on an average of 256 scans at a resolution of 2 cm⁻¹.

Differential scanning calorimetry (DSC) thermograms were obtained on a Perkin-Elmer DSC-7 in a dry nitrogen atmosphere and were used to determine the glass transition temperatures of the polymer blends. The midpoint temperature of the specific heat increase in the glass transition region during a second heat at 10 °C/min was taken as the T_g .

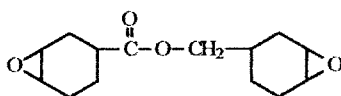
Dynamic mechanical analyses (DMA) were performed at 1 Hz in a Perkin-Elmer DMA-7e with an extension probe at a heating rate of 2 °C/min.

NMR spectra of the polymer blends of BPADA-DAMPO polyimide and PHE were obtained employing a Bruker MSL 300 instrument according to the following procedures: The phosphorus NMR was measured under a standard ³¹P CP-MAS condition, with 100–200 scans per FID using a spinning rate of 6.0–6.5 kHz. Measurements of proton spin–lattice relaxation times in the rotating frame ($T_{1\rho}$) under ¹³C CP-MAS conditions by using a 90° pulse, followed by a variable proton spin lock, followed by a fixed contact time. Twelve proton spin lock periods were used ranging from 0.25 to 20 ms. Measurements of the proton spin–lattice relaxation times in the rotating frame ($T_{1\rho}$) were obtained from a computer-generated best fit of the intensity of the ¹³C NMR spectra to the single-exponential equation $M(t) = M(0) \exp(-t/T_{1\rho})$. All NMR measurements were performed at room temperature with 250–350 mg of sample in a Zirconia rotor with a Kel-F end cap. A 90° pulse of 5 μs was employed with 512 per FID signal accumulations. Spinning rates were 6.0–6.2 kHz, and the Hartmann–Hahn match was adjusted before each accumulation using an adamantane reference sample.

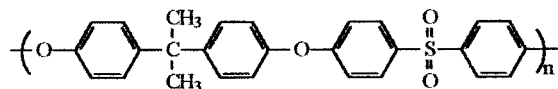
Results and Discussion

Hydrogen Bonding between Phosphonyl and Hydroxyl Groups. Poly(arylene ether phenylphosphine oxide) or Poly(arylene thioether phenylphosphine oxide)/PHE. Hydrogen-bonding interactions in small molecules between the phosphonyl groups and the hydroxyl groups of alcohols, phenols, carboxylic acids, or chloroform have been reported.^{29–33} The association constants for the triphenylphosphine oxide/phenol complex in carbon tetrachloride solvent were reported to be 1055 and 365 at 20 and 50 °C, respec-

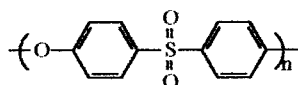
Scheme 2



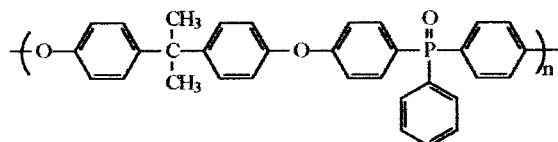
ERL-4221* (3,4-epoxycyclohexylmethyl-3,4-epoxycyclohexyl carboxylate) (ECHMECHC)



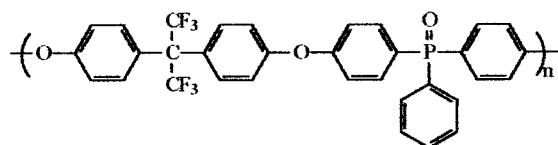
Udel* Bisphenol A Polysulfone



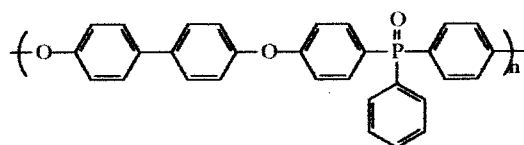
Victrex* Poly(ether sulfone)



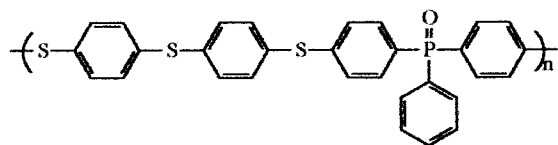
Bisphenol A Poly(arylene ether phenyl phosphine oxide) (BPA-PEPO)



Hexafluorobisphenol A Poly(arylene ether phenyl phosphine oxide) (HFBPA-PEPO)



Biphenol Poly(arylene ether phenyl phosphine oxide) (BP-PEPO)

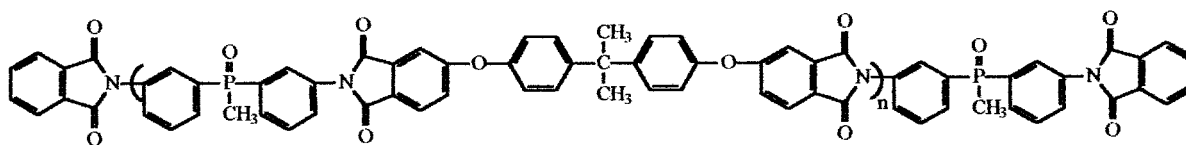


Thiodithiophenol Poly(arylene thioether phenyl phosphine oxide) (SS-PTPO)

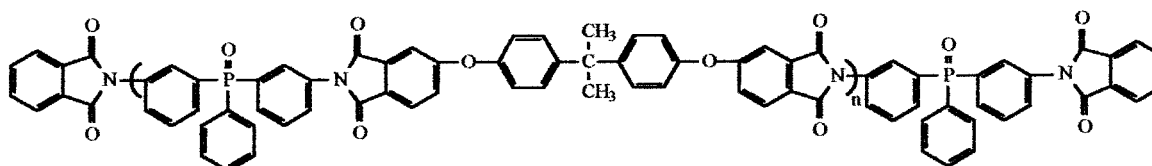
tively.³⁰ This strongly suggests that the driving force for the miscibility of phosphine oxide containing poly(arylene ether)s, and PHE is the hydrogen-bonding interaction.^{17,18} FTIR spectra of bisphenol A poly(arylene

ether phenylphosphine oxide)/PHE showed a shift due to hydrogen bonding of the hydroxyl stretching vibration peak from 3445 to about 3300 cm⁻¹.¹⁸ We previously reported similar hydrogen-bonding interactions between

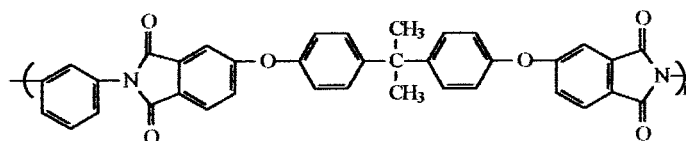
Scheme 3



Polyimide from 2,2'-bis[4-(3,4-dicarboxyphenoxy)phenyl]propane dianhydride (BPADA) and bis(*m*-aminophenyl) methyl phosphine oxide (DAMPO) (BPADA-DAMPO)



Polyimide from 2,2'-bis[4-(3,4-dicarboxyphenoxy)phenyl]propane dianhydride (BPADA) and bis(*m*-aminophenyl) phenyl phosphine oxide (BPADA-DAPPO)



Ultem® (BPADA-*m*-PDA)

bisphenol A poly(arylene ether phosphine oxide) and hydroxyl-containing dimethacrylates.²² This paper describes the hydrogen-bonding interactions observed in the hexafluorobisphenol A and biphenol-based poly(arylene ether phenylphosphine oxide)s. Figure 1a,b shows the stretching vibration of hydrogen-bonded hydroxyl shifted to lower wavenumber.

It was recognized that a significant contribution to hydrogen bonding between the hydroxyl groups of PHE and the ether oxygen atoms of BPA-PEPO could exist. Accordingly, a well-known miscible system poly(ether sulfone) (Vitrex)/PHE was employed as a model system to study the hydrogen-bonding interaction between two components.¹⁶ Figure 2 shows that the peak maximum at 3445 cm⁻¹ due to the stretching vibration of hydrogen-bonded OH of PHE shifted to 3526 cm⁻¹ when PHE was blended with poly(ether sulfone). However, it was not certain whether the shift of hydrogen-bonded OH was due to the interaction of the hydroxyl group with the ether oxygen or the interaction of the hydroxyl group with the sulfonyl group. In either case, the results suggested a quite weak specific interaction because the band attributed to hydrogen-bonded OH stretching vibration shifted to higher wavenumbers.³ The hydrogen-bonding interaction between the hydroxyl group of PHE and the ether group of the phosphorus-containing polymers is thus reasonably assumed to be similar to that observed in the model system; e.g., very weak and negligible. In fact, any hydroxyl/ether oxygen interaction between PHE and another arylene ether polymer would be in direct competition with the hydroxyl/ether oxygen

PHE self-interaction. It is concluded that the strong hydrogen-bonding interaction between phosphonyl groups and hydroxyl groups is the driving force for miscibility in the blends examined in the present research.

The hydrogen-bonded hydroxyl group shifted to low wavenumbers with about the same magnitude as the phosphorus-containing poly(arylene ether)/PHE blend systems in the thioether system, as shown in Figure 3. It is suggested that the thioether sulfur in SS-PTPO should act as a much weaker proton acceptor for hydrogen bonding compared with the ether oxygen, so the predominant contribution of hydrogen bonding should again come from the interaction between hydroxyl and phosphonyl group. These results imply that the hydrogen-bonding interaction between OH and phosphonyl group is relatively independent of the other main-chain molecular features.

Further characterization of the hydrogen bonding was also performed by means of solid-state ³¹P CP-MAS NMR. The ³¹P chemical shift shifted downfield with phosphonyl group hydrogen bonds with other groups. Thus, in the BPA-PEPO/PHE, HFBPA-PEPO/PHE, BP-PEPO/PHE, and SS-PTPO/PHE blend systems, the phosphorus peak shifted from about 25 ppm down to about 29.5 ppm with increasing amounts of PHE in the polymer blends. Parts a and b of Figure 4 show the ³¹P chemical shift in the BPA-PEPO-100/PHE and HFBPA-PEPO/PHE blend systems with various compositions, respectively. Table 2 shows the ³¹P chemical shifts in the various polymer blend systems. The chemical shifts are approximately the same as that of a model

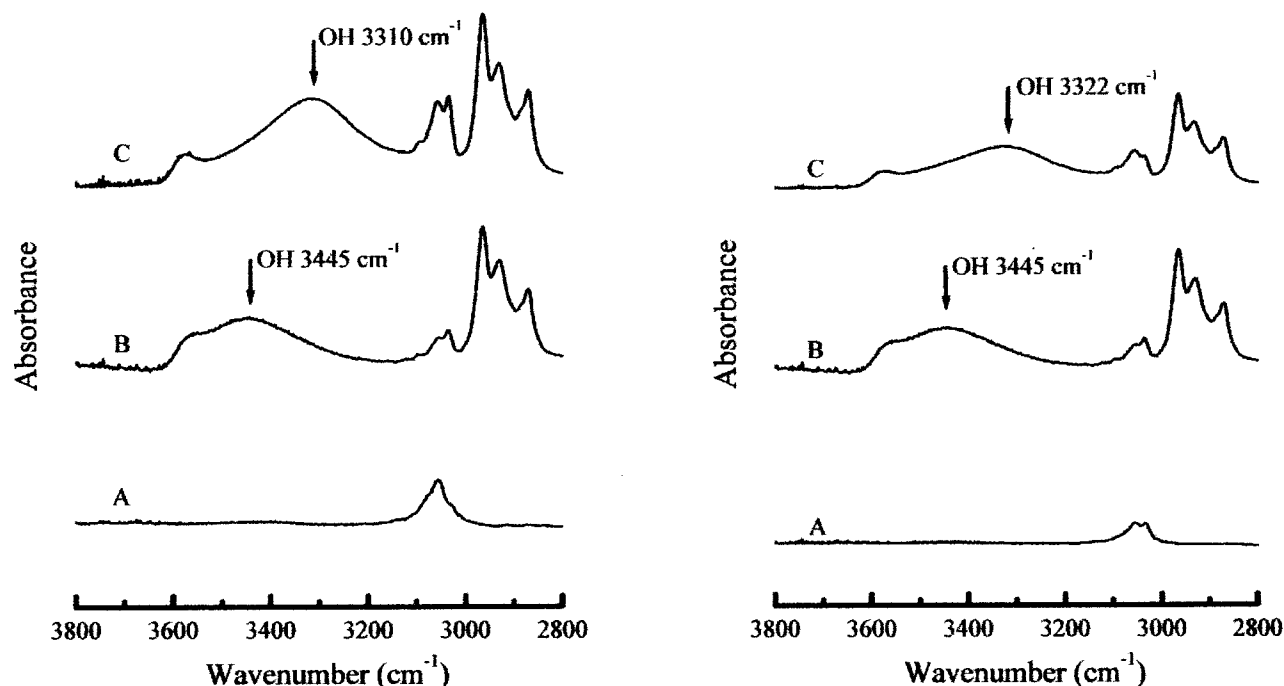


Figure 1. FTIR spectra of (a, left) HFBPA-PEPO/PHE and (b, right) BP-PEPO/PHE blends recorded at room temperature in the hydroxyl stretching region (A) polymer, (B) PHE, and (C) 50/50 wt % blend.

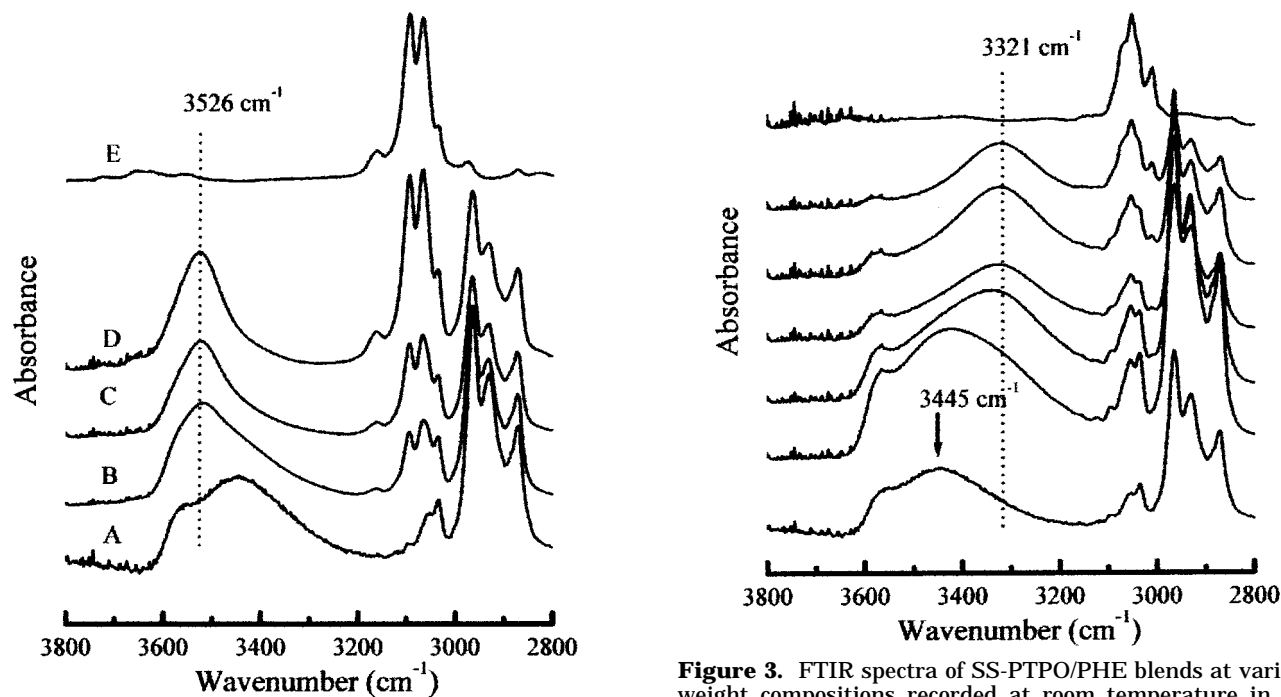


Figure 2. FTIR spectra of poly(ether sulfone)/PHE blends at various compositions (repeat unit mole ratios) recorded at room temperature in the hydroxyl stretching region (A) 0:1, (B) 1:2, (C) 1:1, (D) 2:1, and (E) 1:0.

triphenylphosphine oxide in 2-propanol in 1:20 mole ratio solutions.³² These spectra reveal changes in the chemical shifts that could be a result of specific molecular interactions between blend components. Changes in the chemical shift originate from relatively short-range effects, so they necessarily indicate interaction between the blend constituents on a molecular level. Chemical shift changes may be induced directly by interchain shielding, that is, by alteration of the phosphorus electron cloud by a change in chemical environ-

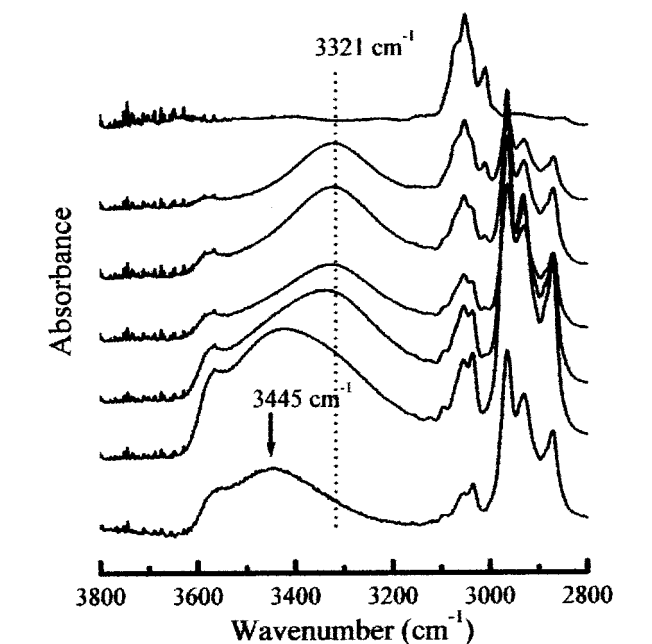


Figure 3. FTIR spectra of SS-PTPO/PHE blends at various weight compositions recorded at room temperature in the hydroxyl stretching region at (A) 0/100, (B) 20/80, (C) 40/60, (D) 50/50, (E) 60/40, (F) 80/20, and (G) 100/0 wt % compositions.

ment, or indirectly by changes in conformation through modification of bond angles and variations in intrachain nearest-neighbor distances.³⁴ The spectral changes shown in Figure 4a,b provide strong evidence for intimate intermixing on a molecular scale.

It should be noted that the chemical shift of phosphorus in a copolymer BPA-PEPO-50 (with 50:50 mole ratio of bis(4-fluorophenyl)phenylphosphine oxide and 4,4'-dichlorodiphenyl sulfone as the comonomers) has the same chemical shift as the homopolymer BPA-PEPO. The BPA-PEPO-50/PHE blends showed the

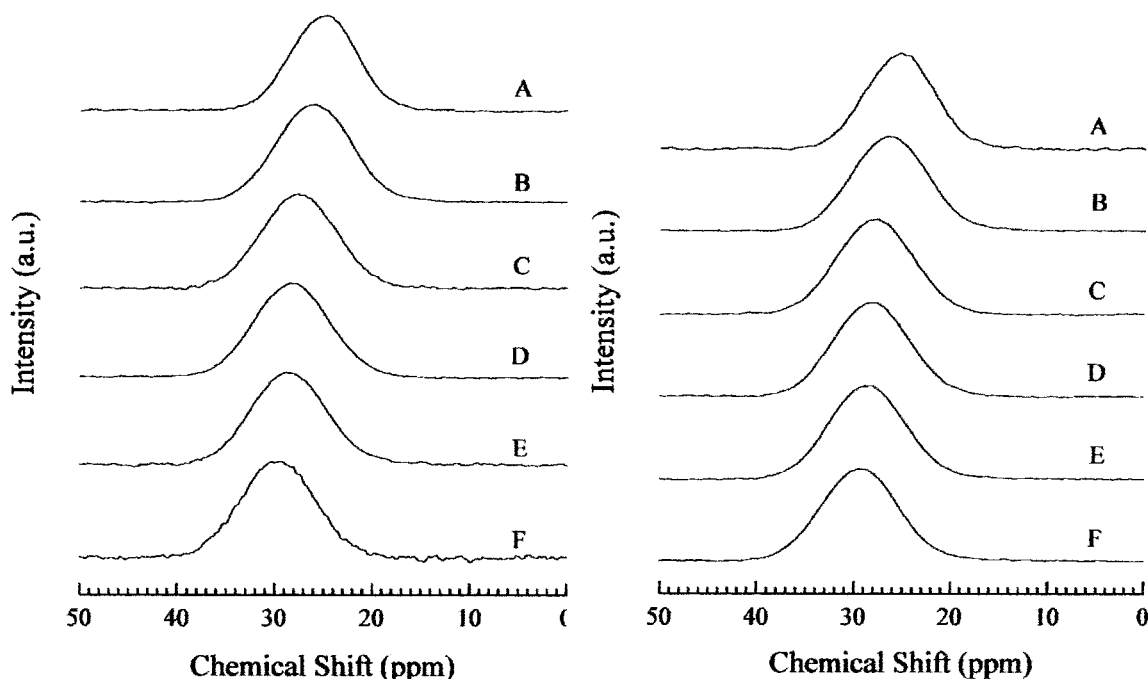


Figure 4. CP-MAS ^{31}P NMR spectra of (a, left) BPA-PEPO/PHE and (b, right) HFBPA recorded at room temperature at (A) 100/0, (B) 80/20, (C) 60/40, (D) 50/50, (E) 40/60, and (F) 20/80 wt % compositions.

Table 2. Chemical Shifts of Solid-State ^{31}P CP-MAS NMR Resonances of Various Polymer Blends

blend	wt % of X-PEPO, SS-PTPO, or X-DAMPO in the Blends for chemical shift (ppm) of					
	0	20	40	50	60	100
BPA-PEPO-100/PHE	29.5	28.9	28.3	27.7	26.2	25.1
BPA-PEPO-50/PHE		29.0	28.3	27.6	26.3	25.0
HFBPA-PEPO/PHE	29.1	28.6	28.1	27.7	26.4	25.2
BP-PEPO/PHE	29.9	29.1	29.0	27.5	26.5	25.8
SS-PTPO/PHE	29.4	29.0	28.5	27.7	26.8	25.7

same tendency as homopolymer BPA-PEPO/PHE, suggesting that the chemical shift is not due to the dilution of phosphonyl groups in the blend systems.³⁵ For the blends with the same weight composition, the chemical shift is approximately the same. This may be explained by the accessibility of phosphonyl groups. Not all of the phosphonyl groups would be expected to be accessible to hydrogen bonding due to steric hindrance considerations.

Further investigation of the origin of the phosphorus chemical shifts of poly(arylene ether phenylphosphine oxide)/PHE systems was attempted by selecting a model system BPA-PEPO/ERL-4221 (3,4-epoxycyclohexylmethyl-3,4-epoxycyclohexyl carboxylate) (ECHM-ECHC), a miscible blend system without hydrogen bonding.³⁶ Figure 5 shows the chemical shift of BPA-PEPO/ERL-4221 blends. Compared with that of BPA-PEPO/PHE, the phosphorus chemical shift only slightly moved downfield with the change of compositions in the BPA-PEPO/ERL-4221 blend system. The results further suggest that the chemical shift of phosphorus is mainly due to the hydrogen bonding with a hydroxyl instead of other effects.

Figure 6 shows the ^{31}P chemical shift of SS-PTPO/PHE blends. As surmised before, the hydrogen bonding between hydroxyl and thioether sulfur should be relatively weaker in the SS-PEPO/PHE blend system, and one concludes the chemical shift of phosphorus is strong evidence of the hydrogen bonding between the phosphonyl groups and hydroxyl groups.

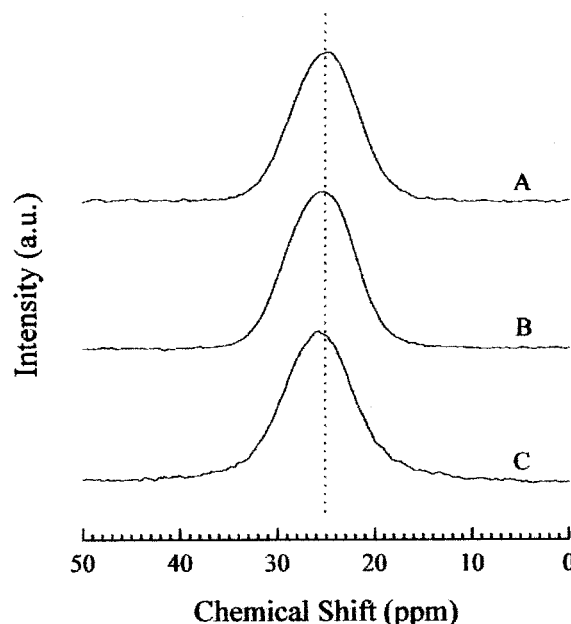


Figure 5. CP-MAS ^{31}P NMR spectra of BPA-PEPO/ERL-4221 recorded at room temperature at (A) 100/0, (B) 60/40, and (C) 40/60 wt % compositions.

Phosphine Oxide Containing Polyimide and Bisphenol A Poly(hydroxy ether)s System (BPADA-DAMPO)/PHE. FTIR spectra of BPADA-DAMPO polyimide, PHE, and their blends are displayed in Figure 7a,b. One notes that the band of the hydroxyl stretching vibration shifted from 3445 to about 3320 cm^{-1} . In contrast, the band due to the carbonyl stretching vibration did not shift, indicating little or no hydrogen-bonding interaction between the carbonyl group of BPADA-DAMPO and the hydroxyl group of PHE. The immiscibility of the BPADA-*m*-PDA resin and PHE provides indirect evidence of minimal interaction between the carbonyl group of polyimide and the hydroxyl group of PHE. The solid-state ^{31}P CP-MAS NMR spectra

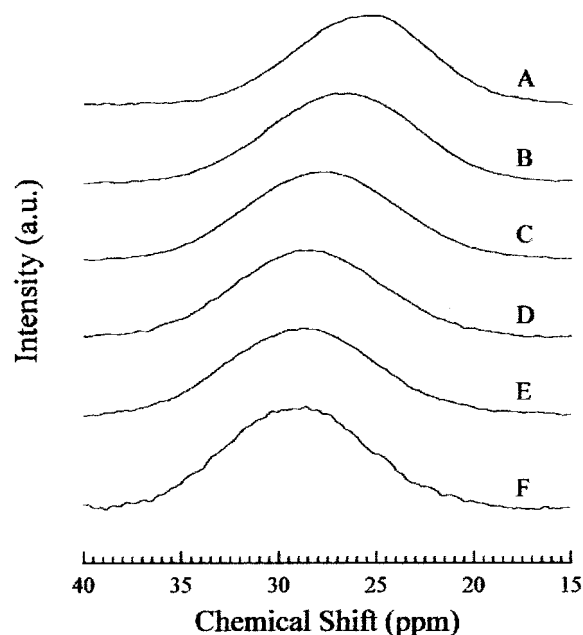


Figure 6. CP-MAS ^{31}P NMR spectra of SS-PTPO/PHE recorded at room temperature at (A) 100/0, (B) 80/20, (C) 60/40, (D) 50/50, (E) 40/60, and (F) 20/80 wt % compositions.

of the blends (BPADA-DAMPO/PHE) show a progressive downfield shift in the chemical shift of phosphorus, as illustrated in Figure 8. The results of FTIR and solid-state NMR measurements suggested hydrogen-bonding interaction between the phosphonyl and hydroxyl groups of the two components.

Miscibility and Glass Transition Temperatures of Polymer Blends. The films of poly(arylene ether phenylphosphine oxide)s, or poly(arylene thioether phenylphosphine oxide), or phosphine oxide-containing polyimides/PHE prepared by either solution casting or melt pressing are transparent, even though their refractive index values are different, suggesting their miscibility. It is recognized that the determination of miscibility may be dependent on the criteria of the physical method employed and that sometimes these criteria may give misleading results.³⁷ Miscibilities of the above polymer blends were thus further characterized by DSC and DMA and a single T_g at a temperature intermediate between those of the pure components indicates miscibility. In the present study, all the samples were completely solvent free as checked by TGA and NMR. The data were collected from second-run DSC scans to minimize thermal history and solvent effects. Parts a and b of Figure 9 display the DSC thermograms of polymer blends at various compositions of HFBPA-PEPO/PHE and BP-PEPO/PHE, respectively. The DSC thermograms show single T_g values for the polymer blends over the entire composition range, and the glass transition temperature increases monotonically with increasing amounts of HFBPA-PEPO or BP-PEPO. DMA also showed a similar increase of the peak temperature of well-defined single $\tan \delta$ loss peaks with increasing amounts of HFBPA-PEPO or BP-PEPO, as shown in Figure 10a,b. These results again strongly support our hydrogen-bonding hypothesis.^{17,18,22}

The single glass transition behavior was also observed in the SS-PTPO/PHE system. Figure 11 illustrates the monotonic increase in T_g with increase in the weight percent of SS-PTPO.

Table 3. Glass Transition Temperatures (DSC) of Polymer Blends of PHE with Various Phosphine Oxide-Containing Polymers

blend	wt % of X-PEPO or SS-PTPO in the blends at T_g (°C) of						
	0	20	40	50	60	80	100
HFBPA-PEPO/PHE	93	111	132	144	170	180	209
BP-PEPO/PHE	93	121	143	157	171	196	234
SS-PTPO/PHE	93	108	126	135	143	160	175
BPADA-DAMPO/PHE	93	120	143	154	164	187	213
BPADA-DAPPO/PHE	93	116	138	150	161	184	213

A totally different system, phosphorus-containing polyimide/PHE blends, was also investigated to expand the breadth of material systems. As an evidence of the miscibility of this system, the films of BPADA-DAMPO/PHE prepared by either solution casting or melt pressing were transparent even though refractive index values were very different for the homopolymers. Further qualitative criteria indicating the miscibility of this blend system were provided by DSC and DMA data. Both DSC and DMA thermograms show single T_g values for the polymer blends over the entire composition range. The glass transition temperatures increased monotonically with the increase of the amount of polyimide. To illustrate this finding, Figure 12a,b shows the DSC and DMA results for BPADA-DAMPO/PHE blends. The DSC and DMA results are consistent. They indicate that the two polymer components are miscible, at least on the scale detectable by DSC and DMA. Further study of the effect of polyimide structure on the miscibility was done (e.g., phenyl vs methyl group) by blending a similar polyimide (BPADA-DAPPO) with PHE. The resulting polymer blends also showed a single T_g . Again, it suggests the determining factor for the miscibility is hydrogen bonding.

In contrast, the blends of commercial BPADA-*m*-PDA (Ultem resin) and PHE did not yield transparent films either by solution casting or melt pressing, although the BPADA-*m*-PDA has a structure somewhat similar to those of the above phosphorus-containing polyimides. In Figure 13, DSC thermograms show two T_g values for the polymer blends corresponding to the T_g values of the homopolymer components. It should be noted that neither the ether oxygen group nor the carbonyl group afforded significant hydrogen bonding with PHE. Thus, BPADA-*m*-PDA is not miscible with PHE. This result indirectly shows the importance of the phosphonyl group for the miscibility of phosphorus-containing polymers with PHE.

One of the most important ways of characterizing miscible polymer blends is the determination of the composition dependencies of their T_g values. The study of the relationship of glass transition temperatures to the composition of mixtures is of both technological and scientific interest. The glass transition temperatures of some polymer blends measured by DSC and DMA are tabulated in Table 3 and Table 4, respectively. For simplicity, only T_g values obtained by DSC will be discussed.

Since the purpose of the present effort was to study the effect of the polymer, main-chain structures of phosphorus-containing polymers on the blend miscibilities, T_g data, as tabulated in Table 3, were examined for five different polymer/PHE blends using four different T_g -weight fraction composition equations.

The first three equations were derived on the bases of free volume additivity [Fox: eq 1],³⁸ free volume

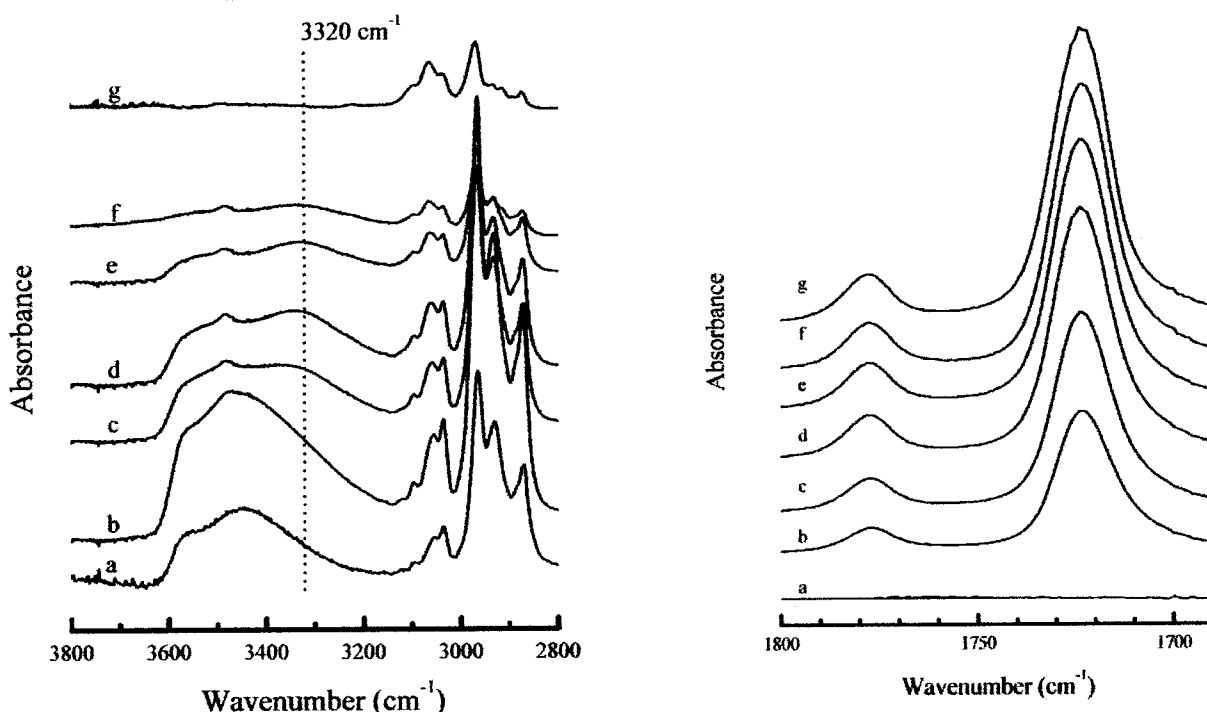


Figure 7. FTIR spectra of BPADA-DAMPO/PHE blends at various weight compositions recorded at room temperature (a, left) in the hydroxyl stretching region and (b, right) in the carbonyl stretching region at (A) 0/100, (B) 20/80, (C) 40/60, (D) 50/50, (E) 60/40, (F) 80/20, and (G) 100/0 wt % compositions.

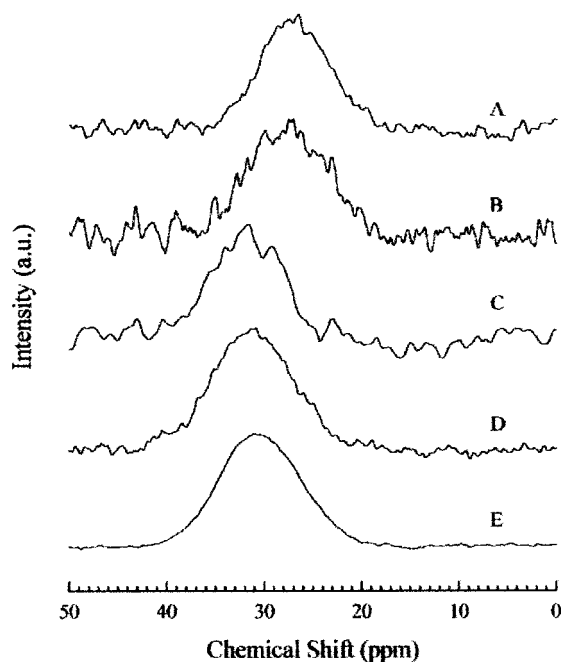


Figure 8. CP-MAS ^{31}P NMR spectra of BPADA-DAMPO/PHE recorded at room temperature at (A) 100/0, (B) 80/20, (C) 60/40, (D) 50/50, and (E) 40/60 wt % compositions.

additivity corrected for thermal expansion coefficient differences [Gordon–Taylor: eq 2],³⁹ or a pseudo-second-order thermodynamic transition combination of entropic changes in the constituent polymers at their respective glass transitions [Couchman: eq 3].⁴⁰ The fourth equation [Kwei: eq 4]⁴¹ is an empirical equation of the Gordon–Taylor form to which a term representing specific interaction contributions has been added. A recent derivation similar in protocol to that of Couchman, but from an enthalpic approach and incorporating

Table 4. Tan δ Peak Values of Polymer Blends HFBPA-PEPO/PHE, BP-PEPO/PHE, and BPADA-DAMPO/PHE

blend	wt % of X-PEPO in the blends at T_g (°C) of						
	0	20	40	50	60	80	100
HFBPA-PEPO/PHE	86	122	145	158	170	189	212
BP-PEPO/PHE	86	126	149	167	182	204	243
BPADA-DAMPO/PHE	86	119	144	155	166	186	208

an enthalpy of mixing, has yielded an equation of the Kwei form expressed, however, in polymer unit mole fractions.⁴²

$$\text{Fox: } \frac{1}{T_{gm}} = \frac{w_A}{T_{gA}} + \frac{w_B}{T_{gB}} \quad (1)$$

$$\text{Gordon–Taylor: } T_{gm} = \frac{w_A T_{gA} + k_{GT} w_B T_{gB}}{w_A + k_{GT} w_B} \quad (2)$$

$$\text{Couchman: } \ln T_{gm} = \frac{w_A \ln T_{gA} + k_C w_B \ln T_{gB}}{w_A + k_C w_B} \quad (3)$$

$$\text{Kwei: } T_{gm} = \frac{w_A T_{gA} + k_K w_B T_{gB}}{w_A + k_K w_B} + q w_A w_B \quad (4)$$

In the Fox equation, the predicted glass transition temperature is dependent only on the weight fraction compositions of the prepared blends and the experimentally determined glass transition temperatures of the constituent polymers. From the derivation of the Gordon–Taylor equation $k_{FT} = (\alpha_{lB} - \alpha_{gB})/(\alpha_{lA} - \alpha_{gA})$ is a compression constant involving the ratio of the thermal expansion coefficient changes of the constituent polymers at their respective glass transitions. The Couchman equation derivation gives $k_C = (C_{lB} - C_{gB})/$

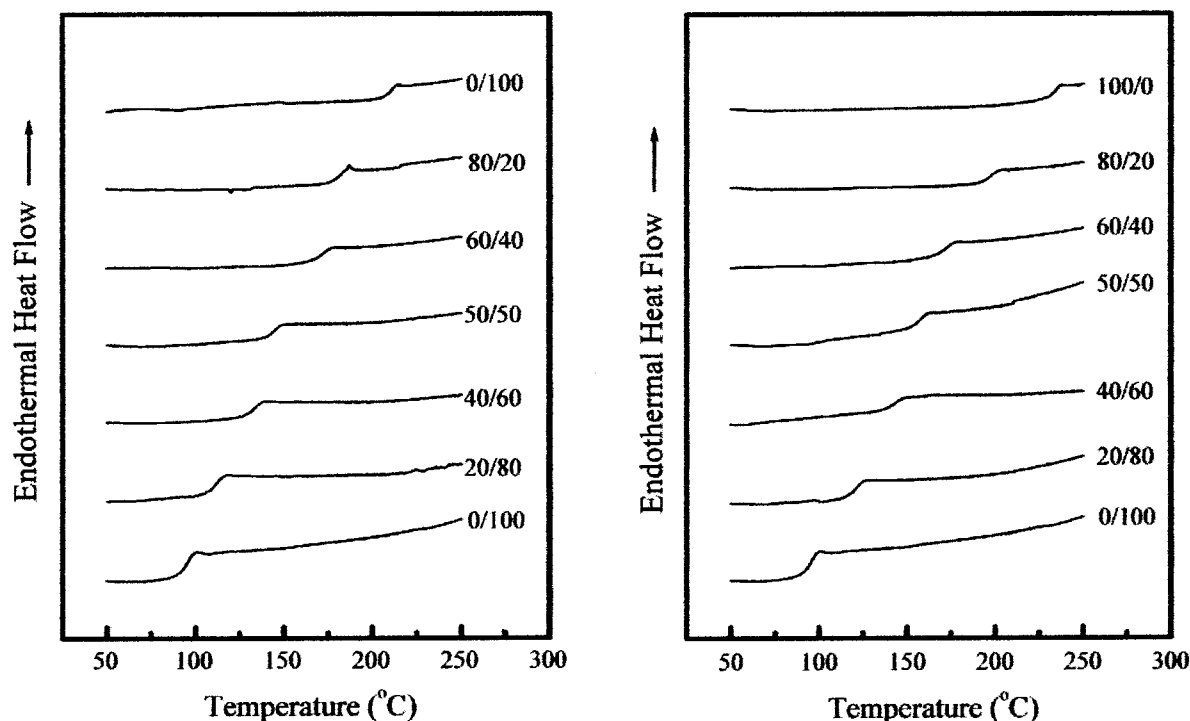


Figure 9. DSC thermograms of (a, left) HFPBA-PEPO/PHE and (b, right) BP-PEPO/PHE blends at various weight compositions.

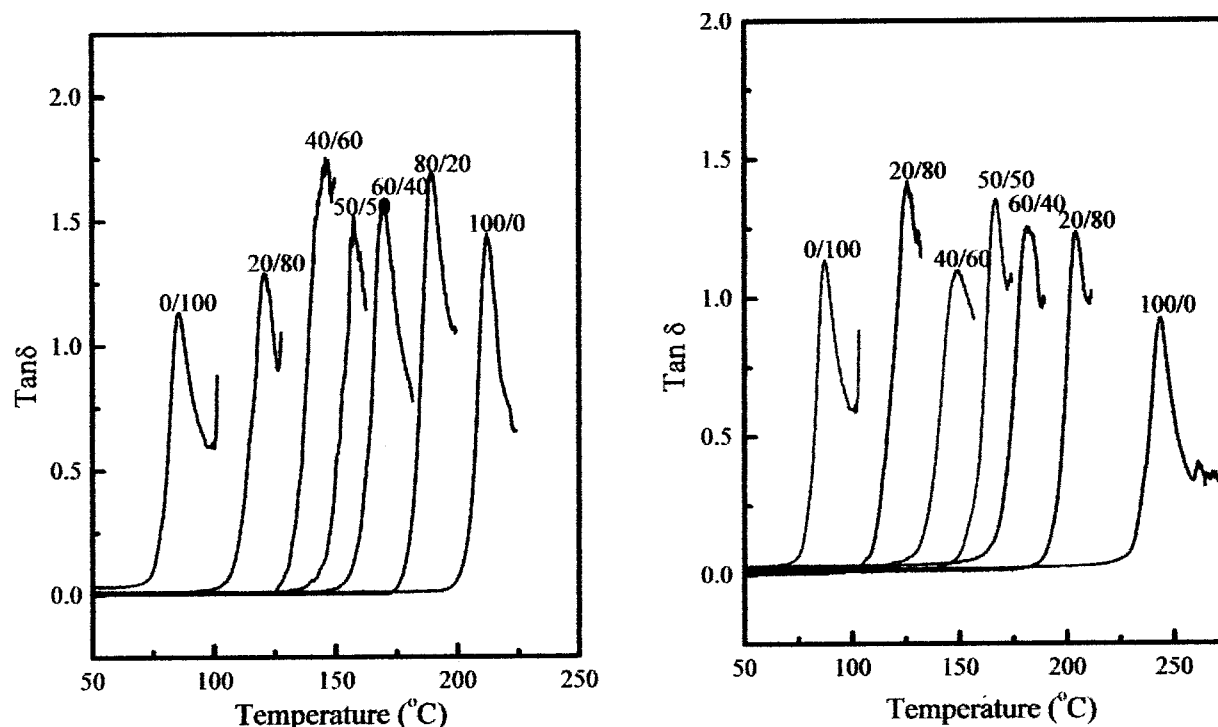


Figure 10. Mechanical loss tangents of (a, left) HFPBA-PEPO/PHE and (b, right) BP-PEPO/PHE blends at various weight compositions.

($C_{lA} - C_{gA}$); the ratio of the specific heat increases of the constituent polymers at their respective glass transitions. The empirical Kwei equation, which has the form of the Gordon–Taylor equation plus an arbitrary “interaction contribution” term, could logically be applied by setting k_K equal to the theoretical k_{GT} and employing q as an adjustable parameter. In T_g data analyses of the composition dependencies of miscible polymer blends k_{GT} and k_C are often treated as adjustable, curve-fitting parameters which contain a combination of the individual constituent contributions and

specific interaction contributions. Adopting such an empirical curve-fitting approach to the present T_g – w data, we obtained the parameter values shown in Table 5. Rather than setting k_K equal to the theoretical k_{GT} as suggested above, k_K is set equal to the theoretical k_C of Couchman in calculating the q values listed in Table 5. The heat capacity increases at T_g are 0.20, 0.20, 0.22, 0.25, and 0.24 J/(g °C) for BFPA-PEPO, BP-PEPO, SS-PTPO, BPADA-DAMPO, and BPADA-DAPPO, respectively. The heat capacity increase at T_g of PHE is 0.41 J/(g °C).

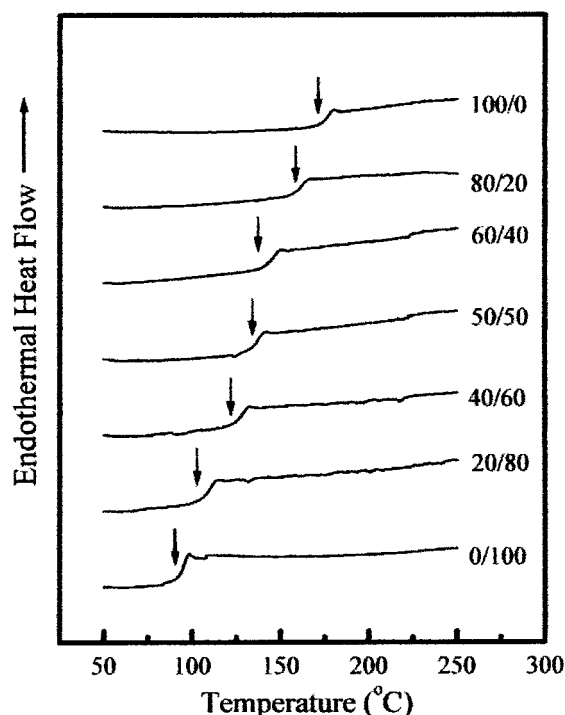


Figure 11. DSC thermograms of SS-PTPO/PHE blends at various weight compositions.

Table 5. Empirical Constants Determined for the T_g /Composition Equations of PHE Blends

blend	k_{GT}		k_C		q (°C)	
	DSC	DMA	DSC	DMA	DSC	DMA
HFBPA-PEPO/PHE	0.74	1.1	1.1	1.6	53	120
BP-PEPO/PHE	0.82	0.74	1.2	1.3	70	108
SS-PTPO/PHE	1.20		1.1		53	
BPADA-DAMPO/PHE	0.89	1.1	1.0	1.5	60	93
BPADA-DAPPO/PHE	0.78		0.89		48	

Figure 14 presents the observed T_g values of HFBPA-PEPO/PHE, SS-PTPO/PHE, and BPADA-PEPO/PHE blends plotted against the weight fractions of the corresponding phosphine oxide containing polymers, representing three totally different kinds of polymer. The positive deviation of the blend T_g relative to the Fox equation prediction (broken line) is observed for all the studied polymer blends. These observations are consistent with a free volume decrease with resultant increased T_g in the blends due to favorable (exothermal, densifying) phosphonyl/hydroxyl group interactions. The deviation of the observed T_g from the theoretical T_g for the HFBPA-PEPO/PHE blend system is relatively smaller, although strong hydrogen-bonding interaction was observed by FTIR and ^{31}P NMR. A possible explanation can be made as follows. Incorporating the relatively bulky CF_3 groups in the chain unit may result in producing a more open polymer chain. Therefore, the hydrogen-bonded polymer blends containing the hexafluoroisopropylidene may possess larger free volume than those of the other polymer blend systems. The result is that the polymer blends are closer to the free-volume additivity condition. Quantitative comparison among the different polymer blend systems is not possible, since both the specific interaction and the chain structure may affect miscibility. Fitting the data to the Gordon–Taylor equation (solid curves in Figure 14) by an adjustable k_{GT} is fairly successful.

Figure 15 presents the same blend glass transition temperature data that were presented in Figure 14, where the broken line curves correspond to the Couchman equation in which k_C values were calculated from the individual constituent polymer specific heat changes at their glass transitions. The solid curves represent the fit using adjustable k_C values. The increased T_g values relative to the theoretical Couchman equation prediction, with the incorporation of phosphine oxide content, are consistent with favorable (exothermal, densifying) phosphonyl/hydroxyl group interactions.

Figure 16 presents the blend T_g data, the T_g values predicted by the theoretical Gordon–Taylor equation (with $k_{GT} = k_C$) represented by broken line curves, and the empirical Kwei equation fit (solid curves) of the data. Fitting the blend T_g data by the Kwei equation with q as an adjustable interaction parameter gives very good fits (solid line curves) with changes of q values in different systems, as tabulated in Table 5. This trend in enhancement of T_g by the $q_{WA}W_B$ term is definitely consistent with a favorable, hydrogen-bonding interaction between the phosphonyl group of the polymer and the hydroxyl group of PHE.

Scale of the Miscibility of BPADA-DAMPO/PHE.

The properties of the polymer blends are of course dependent on their microstructures. Although DSC and DMA can afford some information on the homogeneity of the polymer blends, the information may be on a relatively larger phase scale. Thus, it was of interest to study the polymer blends ^{13}C CP-MAS NMR which provides the possibility of evaluating the scale of miscibility of polymer blends according to the dynamic NMR relaxation measurement.^{34,43–50} The interaction of the blend components by hydrogen bonding has been shown to cause changes in line shape and/or shifts in the ^{13}C resonance frequencies in the NMR spectra of the blend components, in comparison with the spectra of the pure polymer components.^{12c,51} As discussed above, the hydrogen-bonding interactions between phosphorus-containing polymers and PHE cause significant shifts in the ^{31}P NMR resonance frequency. This suggests an intimate interaction between the two components with small domain size. In polymer blends the values of the proton rotating frame spin–lattice relaxation time $T_{1\rho}(H)$ are enhanced by the efficiency of spin diffusion among protons of the polymer components. This efficiency depends on short-range spatial proximity of neighboring chains with different chemical units. In a miscible binary polymer blend, the protons of the two components are closely coupled and expected to relax at an identical rate.^{44,48,52} The relaxation measurements provide miscibility information on a very fine scale. Unfortunately, this method can only be applied to the BPADA-DAMPO/PHE blends in our study due to the overlapping of the spectra of the two components in other systems mentioned above. Even in this system, only $T_{1\rho}(H)$ measurement is available because the two components have similar T_1 values. The peak at 70 ppm has been ascribed to aliphatic CH_2 and CH carbons.^{12c} The 165 ppm resonance peak has been ascribed to carbonyl carbon. Initial measured spin–lattice relaxation times in the rotating frame ($T_{1\rho}(H)$) for the homopolymers and blends are shown in Table 6. In all the blends with various compositions, the $T_{1\rho}(H)$ values of both components are approximately the same.

If the motion of the polymer components in the blends is not greatly changed by blending, the average proton

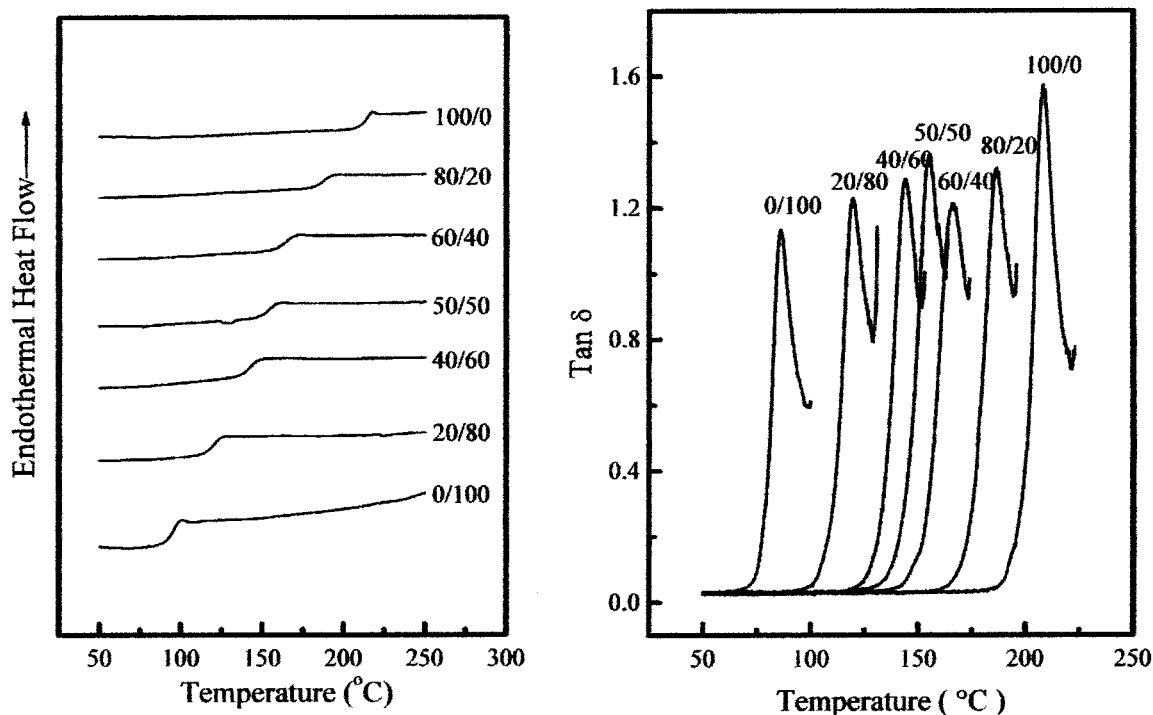


Figure 12. DSC thermograms (a, left) and mechanical loss tangents (b, right) of BPADA-DAMPO/PHE at various weight compositions.

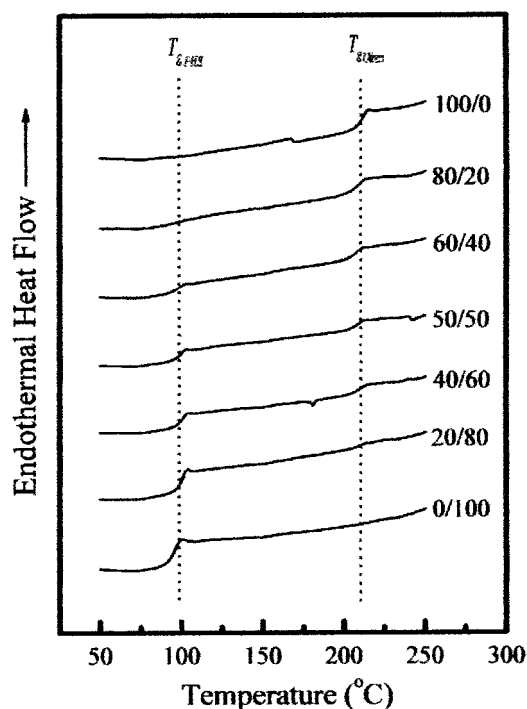


Figure 13. DSC thermograms of BPADA-*m*-PDA/PHE at various weight compositions.

relaxation rate (the inverse of the relaxation time) of a homogeneous blend can be predicted by the model for linear additivity of relaxation times of pure components:^{35,53}

$$\frac{1}{T_{1\rho}(H)_{AB}} = \frac{N_A}{N} \frac{1}{T_{1\rho}(H)_A} + \frac{N_B}{N} \frac{1}{T_{1\rho}(H)_B} \quad (5)$$

where $1/T_{1\rho}(H)_A$, $1/T_{1\rho}(H)_B$, and $1/T_{1\rho}(H)_{AB}$ are the relaxation rates of polymer A, polymer B, and their

Table 6. $T_{1\rho}(H)$ Values (ms) for PHE, BPADA-DAMPO, and Their Blends^a

BPADA-DAMPO/PHE (wt %)	BPADA-DAMPO 165 ppm	PHE 70 ppm	calcd value
0/100		2.04	2.04
20/80	2.24	2.59	2.25
40/60	3.03	3.12	2.56
50/50	3.45	2.84	2.78
60/40	2.73	3.51	3.07
80/20	5.31	4.46	4.07
100/0	6.92		6.92

^a Accuracy of the measurements is about $\pm 10\%$.

blends, respectively; N_A , N_B , and N_{AB} are the numbers of protons of the respective components and for the polymer blends $N_{AB} = N_A + N_B$. The calculated values of the polymer blends are tabulated in Table 6. It is noted that there is a positive deviation of the experimental results from the calculated values. Hydrogen bonding apparently makes the chains stiffer and hinders the segmental motion of the components. Thus, a slower spin-lattice relaxation rate was observed.

The approximate scale of mixing can be readily calculated with the equation $L^2 \approx L_0^2 t/T_2$, where L_0 is the distance between protons, typically 0.1 nm, t the measured relaxation time, and T_2 the spin-spin relaxation time which, below T_g , is ca. $10 \mu s$.⁵² Therefore, from the $T_{1\rho}(H)$ values, it is estimated that BPADA-DAMPO polyimide and PHE mix on a scale of about 3–4 nm.

A one-dimensional diffusion equation for the average diffusive path length can also be used to estimate the mixing scale.^{45,54}

$$L = \sqrt{6DT_i} \quad (6)$$

where D is the spin-diffusion coefficient that depends on the average proton to proton distance as well as on dipolar interactions with a typical value of the order of $6 \times 10^{-16} \text{ m}^2 \text{ s}^{-1}$. T_i is the relaxation time according to

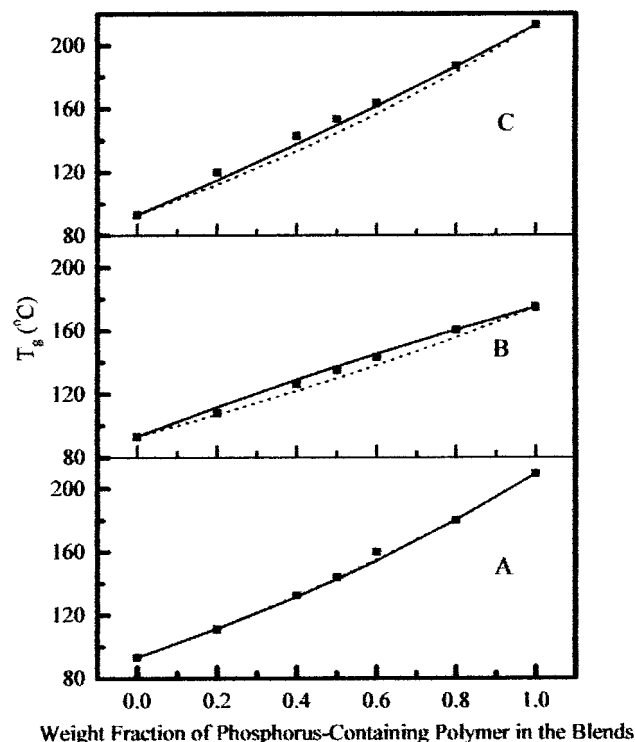


Figure 14. Fit of experimental T_g vs composition data to the curves predicted by the Fox equation (broken line) and the Gordon–Taylor equation with empirically adjusted k_{CT} (solid line): (A) HFBPA-PEPO/PHE, (B) SS-PTPO/PHE, and (C) BPADA-PEPO/PHE.

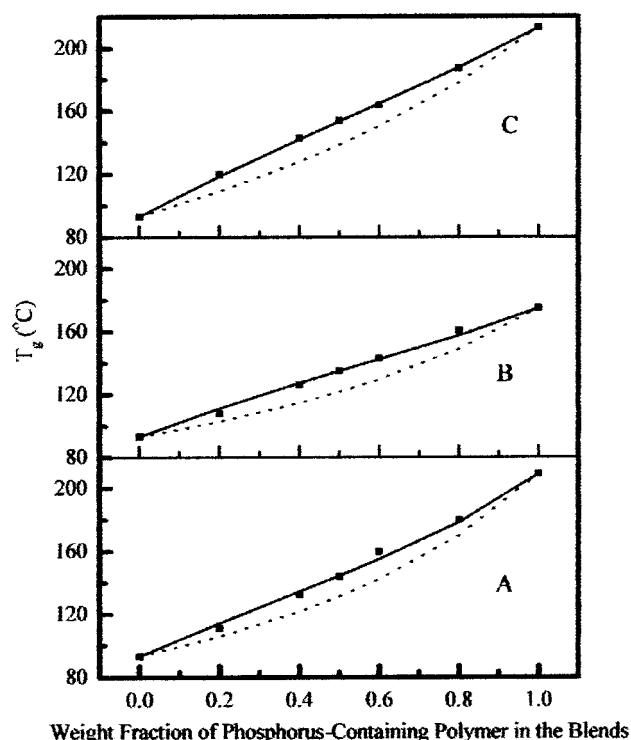


Figure 16. Fit of experimental T_g values to those predicted by the Gordon–Taylor part term of the Kwei equation with $k_K = k_C$ (broken line) and the full form of Kwei equation (solid line): (A) HFBPA-PEPO/PHE, (B) SS-PTPO/PHE, and (C) BPADA-PEPO/PHE.

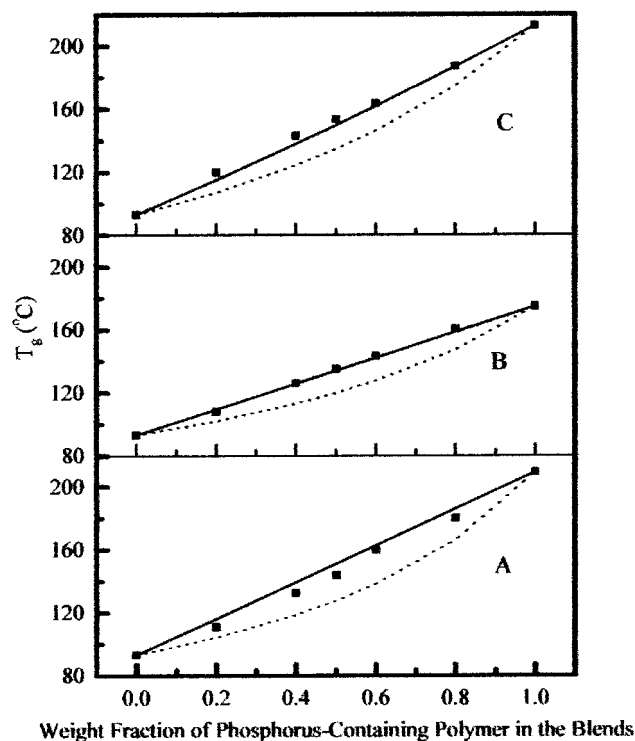


Figure 15. Fit of experimental T_g values to those predicted by Couchman with k_C as the ratio of the heat capacity increases of the components at their T_g (broken line) and with empirical k_C (solid line): (A) HFBPA-PEPO/PHE, (B) SS-PTPO/PHE, and (C) BPADA-PEPO/PHE.

the relaxation experiment. The estimated mixing scale is about 4 nm, which is consistent with the previous equation.

Conclusions

It has been demonstrated that a new series of phosphine oxide-containing poly(arylene ether)s (BPA-PEPO, HFBPA-PEPO, BP-PEPO), poly(arylene thioether phenylphosphine oxide) (SS-PTPO), and polyimides (BPADA-DAMPO, BPADA-DAPPO) are miscible with PHE on the basis of optical clarity and DSC and DMA data. Both DSC and DMA results show single composition-dependent T_g 's for the polymer blends. The glass transition temperatures of the polymer blends were intermediate between those of the pure components and varied monotonically with the blend compositions. It is suggested that the intermolecular hydrogen bonding of phosphonyl groups with hydroxyl groups is the driving force for the miscibility. Several pieces of evidence support the hydrogen-bonding hypothesis. It was observed that the FTIR band due to the hydrogen-bonded hydroxyl stretching vibration shifts from about 3445 to about 3300 cm^{-1} in phosphorus-containing polymers/PHE blends systems while that of a control poly(ether sulfone)/PHE blends shifts to a higher wave-number. This is because these miscible polymer blends are induced by different hydrogen-bonding interactions. Furthermore, this shift is observed in SS-PTPO (without an ether group)/PHE and BPADA-DAMPO/PHE in which no carbonyl stretching vibration band shift is observed. In addition, solid-state ^{31}P CP-MAS NMR spectra show a significant downfield shift of the phosphorus resonance band in phosphorus-containing polymer/PHE blends while it does not display a significant phosphorus chemical shift in a miscible blend BPA-PEPO/ERL 4421.

Evidence for miscibility in BPADA-DAMPO/PHE blends is also obtained from spin–lattice relaxation ($T_{1\rho}(H)$) measurements. From solid-state NMR relax-

ation measurements the homogeneity scale of the different blends was evaluated, and the proximity of different chains is approximately within 4 nm. These results further suggest that varying the main-chain structural units of the phosphorus-containing polymer does not significantly affect its miscibility with PHE resin.

Acknowledgment. The authors thank the Office of Naval Research, under ONR Contract N00014-91-J-1037, as well as the Omnova Foundation, for support of this research effort.

References and Notes

- (1) Olabisi, O.; Robeson, L. M.; Shaw, M. T. *Polymer-Polymer Miscibility*; Academic Press: New York, 1979.
- (2) (a) Paul, D. R.; Newman, S. *Polymer Blends*; Academic Press: New York, 1978; Vols. I and II. (b) Paul, D. R.; Bucknall, C. *Polymer Blends*; John Wiley & Sons: New York, 2000; Vols. I and II.
- (3) Coleman, M. M.; Graf, J. F.; Painter, P. C. *Specific Interactions and the Miscibility of Polymer Blends*; Technomic: Lancaster, PA, 1991.
- (4) Utracki, L. A. *Polymer Alloy and Blends*; Hanser Publishers: Munich, 1989.
- (5) Brode, G. L.; Koleske, J. V. *J. Macromol. Sci., Chem.* **1972**, *6*, 1109.
- (6) Robeson, L. M.; Furtak, A. B. *J. Appl. Polym. Sci.* **1979**, *23*, 645.
- (7) Seefried, C. G., Jr.; Koleske, J. V.; Critchfield, F. E. *Polym. Eng. Sci.* **1976**, *16*, 771.
- (8) Paul, D. R.; Barlow, J. W. *J. Macromol. Sci., Rev. Macromol. Chem.* **1980**, *C18*, 109.
- (9) Smith, K. L.; Winslow, A. E.; Petersen, D. E. *Ind. Eng. Chem.* **1959**, *51*, 1361.
- (10) (a) Robeson, L. M.; Hale, W. F.; Merriam, C. N. *Macromolecules* **1980**, *14*, 1644. (b) Osada, Y.; Sata, M. *J. Polym. Sci., Polym. Lett. Ed.* **1976**, *14*, 129. (c) Coleman, M. M.; Moskala, E. *J. Polymer* **1983**, *24*, 251.
- (11) (a) Chiou, J. S.; Paul, D. R. *J. Appl. Polym. Sci.* **1991**, *42*, 8131. (b) Soh, Y. S. *J. Appl. Polym. Sci.* **1992**, *45*, 8131. (c) Ward, Y.; Mi, Y. *Polymer* **1999**, *40*, 2465.
- (12) (a) Eguiazable, J. I.; Iruin, J. J.; Cortazer; Guzman, G. M. *Makromol. Chem.* **1984**, *185*, 1761. (b) Martinez de Ilarduya, A.; Iruin, J. J.; Fernandez-Berridi, M. J. *Macromolecules* **1995**, *28*, 3707. (c) Zheng, S.; Guo, Q.; Mi, Y. *J. Polym. Sci., Polym. Phys. Ed.* **1998**, *36*, 2291.
- (13) Guo, Q.; Huang, J.; Chen, T. *Polym. Bull.* **1988**, *20*, 517.
- (14) Dai, J.; Goh, S. H.; Lee, S. Y.; Siow, K. S. *Polymer* **1996**, *37*, 3259.
- (15) Lau, C.; Zheng, S.; Zhong, Z.; Mi, Y. *Macromolecules* **1998**, *31*, 7291.
- (16) (a) Singh, V. B.; Walsh, D. J. *J. Macromol. Sci., Phys.* **1986**, *B25*, 65. (b) Reimers, M. J.; Barbari, T. A. *J. Polym. Sci., Polym. Phys.* **1994**, *32*, 131.
- (17) Srinivasan, S.; Kagumba, L.; McGrath, J. E. *Macromol. Symp.* **1997**, *122*, 95.
- (18) Wang, S.; Ji, Q.; Tchatchoua, C. N.; Shultz, A. R.; McGrath, J. E. *J. Polym. Sci., Polym. Phys. Ed.* **1999**, *37*, 1849.
- (19) Guo, Q. *Polymer* **1995**, *36*, 4753.
- (20) Sun, J.; Cabasso, I. *J. Polym. Sci., Polym. Chem. Ed.* **1989**, *27*, 3985.
- (21) Zhuang, H.; Pearce, E.; Kwei, T. K. *Macromolecules* **1994**, *27*, 6398.
- (22) Wang, S.; Wang, J.; Ji, Q.; Shultz, A. R.; Ward, T. C.; McGrath, J. E. *J. Polym. Sci., Polym. Phys. Ed.* **2000**, *38*, 2409.
- (23) Lesko, J. J.; Swain, R. E.; Cartwright, J. M.; Chin, J. W.; Reifsnider, K. L.; Dillard, D. A.; Wightman, J. P. *J. Adhes.* **1994**, *45*, 43.
- (24) (a) Smith, C. D. Ph.D. Dissertation, Virginia Polytechnic Institute and State University, Blacksburg, VA, 1991. (b) Smith, C. D.; Grubbs, H. J.; Webster, H. F.; Gungör, A.; Wightman, J. P.; McGrath, J. E. *High Perform. Polym.* **1991**, *4*, 211. (c) Riley, D. J.; Gungör, A.; Srinivasan, S. A.; Sankarapandian, M.; Tchatchoua, C. N.; Muggli, M. W.; Ward, T. C.; McGrath, J. E.; Kashiwagi, T. *Polym. Eng. Sci.* **1997**, *37*, 150. (d) Wang, S. Ph.D. Dissertation, Virginia Polytechnic Institute and State University, Blacksburg, VA, 2000.
- (25) Liu, Y. Ph.D. Dissertation, Virginia Polytechnic Institute and State University, Blacksburg, VA, 1998.
- (26) (a) Tan, B.; Tchatchoua, C. N.; Dong, L.; McGrath, J. E. *Polym. Adv. Technol.* **1998**, *9*, 84. (b) Zhuang, H. Ph.D. Dissertation, Virginia Polytechnic Institute and State University, Blacksburg, VA, 1998.
- (27) Abed, J. C.; Mercier, R.; McGrath, J. E. *J. Polym. Sci., Polym. Chem. Ed.* **1997**, *35*, 977.
- (28) (a) Konas, M.; Moy, T. M.; Rogers, M. E.; Shultz, A. R.; Ward, T. C.; McGrath, J. E. *J. Polym. Sci., Polym. Phys. Ed.* **1995**, *33*, 1429. (b) Konas, M.; Moy, T. M.; Rogers, M. E.; Shultz, A. R.; Ward, T. C.; McGrath, J. E. *J. Polym. Sci., Polym. Phys. Ed.* **1995**, *33*, 1441.
- (29) Hadzi, D. *J. Chem. Soc.* **1962**, 5128.
- (30) Aksnes, G.; Gramstad, T. *Acta Chem. Scand.* **1960**, *14*, 1485.
- (31) Gramstad, T. *Acta Chem. Scand.* **1961**, *15*, 1337.
- (32) Maciel, G. E.; James, R. V. *Inorg. Chem.* **1964**, *3*, 1650.
- (33) Hays, H. R.; Peterson, D. J. In *Organic Phosphorus Compounds*; Kosolapoff, G. M.; Maier, L., Eds.; Wiley-Interscience: New York, 1972; Vol. 3.
- (34) Masson, J.-F.; Manley, R. St. *J. Macromolecules* **1992**, *25*, 589.
- (35) Assink, R. A. *Macromolecules* **1978**, *11*, 1233.
- (36) It was found that BPA-PEPO/4221 is a miscible blend system. Further study of this system is on going and will be reported in later publications.
- (37) MacKnight, W. J.; Karasz, F. E. In *Polymer Blends*; Paul, D. R., Newman, S., Eds.; Academic Press: New York, 1978; Vol. 1.
- (38) Fox, T. G. *Bull. Am. Phys. Soc.* **1956**, *1*, 123.
- (39) Gordon, M.; Taylor, J. S. *J. Appl. Chem.* **1952**, *2*, 493.
- (40) Couchman, P. R. *Phys. Lett.* **1979**, *70A*, 155.
- (41) Kwei, T. K. *J. Polym. Sci., Polym. Lett. Ed.* **1984**, *22*, 307.
- (42) Painter, P. C.; Graf, J. F.; Coleman, M. M. *Macromolecules* **1991**, *24*, 5630.
- (43) Stejskal, E. O.; Schaefer, J.; Sefcik, M. D.; McKay, R. A. *Macromolecules* **1981**, *14*, 275.
- (44) Dickson, L. C.; Yang, H.; Chu, C.-W.; Stein, R. S.; Chien, J. C. W. *Macromolecules* **1987**, *20*, 1757.
- (45) Schaefer, J.; Sefcik, M. D.; Stejskal, E. O.; McKay, R. A. *Macromolecules* **1981**, *14*, 188.
- (46) Tekely, P.; Laupretre, F.; Monnerie, L. *Polymer* **1985**, *26*, 1081.
- (47) Gobbi, G. C.; Silvestri, R.; Russell, T. P.; Lyster, J. R.; Fleming, W. W.; Nishi, T. *J. Polym. Sci., Polym. Lett.* **1987**, *25*, 61.
- (48) Grobelny, J.; Rice, D. M.; Karasz, F. E.; MacKnight, W. J. *Macromolecules* **1990**, *23*, 22139.
- (49) Sankarapandian, M.; Kishore, K. *Polymer* **1996**, *37*, 2957.
- (50) Zheng, S.; Guo, Q.; Mi, Y. *J. Polym. Sci., Polym. Phys. Ed.* **1998**, *36*, 2291.
- (51) Qin, C.; Pires, A. T. N.; Belfiore, L. A. *Macromolecules* **1991**, *24*, 666.
- (52) McBrierty, V. J.; Douglass, D. C. *J. Polym. Sci., Macromol. Rev.* **1981**, *16*, 295.
- (53) Schaefer, J.; Stejskal, E. O. *J. Chem. Soc.* **1976**, *98*, 1031.
- (54) (a) McBrierty, V. J.; Douglass, D. C. *Phys. Rep.* **1980**, *63*, 61. (b) McBrierty, V. J.; Packer, K. J. *Nuclear Magnetic Resonance in Solid Polymers*; Cambridge University Press: Cambridge, UK, 1993.

MA001821R